Determination of the Rheological Model of Gel Propellant and Flow Characterization of Gel in a Pressure Swirl Injector

Saberi Moghaddam, Al*+; Mansourizadeh, Farhad; Bahri Rasht Abadi, Mohammad Mahdi

Department of Chemistry and Chemical Engineering, Malek-Ashtar University of Technology, I.R. IRAN

Valizadeh, Esmail

Department of Aero Space Engineering, K. N. Toosi University of Technology, I.R. IRAN

ABSTRACT: *Gel propellants have the advantages of both liquid and solid propellants and present a promising future for the aerospace industry. Many gel propellants have shear-thinning behavior, which complicates their behavior in propulsion systems, especially the atomization process. On the other hand, the toxicity of many gel propellants makes the study of their dynamic behavior difficult. In the present work, non-toxic gel simulants were first prepared using a variety of gelling agents. Next, a gel simulant with a behavior similar to UDMH's basic gel fuel was selected from the prepared simulants. The dynamic behavior of the selected simulant gel was studied by different shear-thinning fluid models, and the most suitable rheological model was chosen. Eventually, the simulant gel dynamic behavior was simulated in a pressure swirl injector using the selected rheological model, and the results were compared to the experimental data. The results indicated that the simulant gel made from 0.85 wt.% of HPMC gelling agent is very similar to the basic UDMH gel in terms of dynamic behavior and power law index. Furthermore, among the rheological models, the Carreau-Yasuda model was able to predict the selected gel simulant behavior in a wide range of shear rates. A comparison of the experimental tests and numerical simulation of the gel simulant flow inside the swirl injector revealed that using the calculated constants of the Carreau-Yasuda model can predict the simulant gel dynamic behavior and the functional characteristics such as mass flow rate, discharge coefficient, and spray cone angle with less than 6% error.*

KEYWORDS*: Gel propellant; Shear-thinning; Atomization; Carreau-Yasuda; Swirl injector; Simulation.*

INTRODUCTION

Gelled propellants include liquid fuel and oxidizers whose rheological behavior changes by adding a gelling agent. It is claimed that gel propellants have the advantages of common liquid and solid propellants, simultaneously, but they do not have the disadvantages of these propellants [1, 2]. Unsymmetrical dimethyl

**To whom correspondence should be addressed.*
+ *E-mail: articlemut@gmail.com*
1021-9986/2023/10/3467-3479 13/$/6.03

hydrazine (UDMH) gel fuel has viscoplastic behavior that under high shear rates, the viscosity of the UDMH gel approaches the viscosity of the UDMH liquid [3, 4]. Having viscoplastic behavior enables the gel to have advantages such as safety, the possibility of long-term storage, and the loading of high-energy particles. Additionally, the gel propulsion systems have thrust control specifications similar to liquid propulsion systems [5, 6]. One of the major challenges of the gel propulsion systems is the atomization of the gelled propellant. The reason is the non-Newtonian behavior and higher viscosity of the gelled propellant compared to the mother liquid propellant. In general, the mother liquid propellant has a low viscosity which is increased by adding the gelling agent to it. This variable property is the reason for the complicated behavior of a gel propellant compared to its mother propellant [7, 8]. Many gel fuels have a shear-thinning behavior in a dynamic state (reduced viscosity by increased shear rate) [9]. Since gel fuels have non-Newtonian behavior, a comprehensive knowledge of the gel propellants' rheological behavior is essential in designing their propulsion systems. The yield stress or the elasticity behavior of a gel fuel plays an important role in storage, transportation, loading of the high energy particles, leakage prevention, and the intensity of shear-thinning behavior in the dynamic and flow state of the gel fuel [5, 10]. The motor section of the gel propulsion system which includes flowing and spraying of gel fuel depends on the dynamic behavior of gel fuel. On the other hand, considering the shear-thinning behavior of the gel fuel, some considerations should be taken into account to reduce pressure drop and improve the atomization process of the gel propellant [5, 11].

Madlener and Ciezki [12] investigated the rheological and flow behavior of gel fuels JetA-1, paraffin, and ethanol aiming to use them in propulsion systems. Mineral and organic gallants are used in this investigation. Their test results indicated that at low to moderate shear rates, the prepared gel fuels have shear-thinning behavior. However, at higher shear rates, the slope of the viscosity curve decreases for all evaluated gel fuels, and gel fuel viscosity approaches to the viscosity of the mother liquid fuel. Furthermore, it was demonstrated that as shear stress increases, the velocity profile of the prepared gel fuels exhibits shear-thinning behavior while transferring through the pipe with a constant cross-section. However, plug flow is formed in the middle part of the pipe due to the low shear rate at initial shear stress values. *Jyoti et al.* [13] compared the rheological characteristics of the ethanol and UDMH-based gel at different temperatures in the range of shear rate (1-12 1/s) based on the power law model. They showed that at an identical percentage of methylcellulose (MC) gellant, the initial viscosity of ethanol gel is higher than UDMH. Furthermore, the results indicated that the shear-thinning behavior of ethanol gel is more than UDMH gel, and the intensity of shear-thinning behavior decreases with temperature increase in both gel fuels. *Rahimi et al*. [2] investigated the rheological behavior of the gel simulants prepared from carbopol and water using the power law and Herschel-Bulkley models. The results indicated that at low shear rates, the Herschel-Bulkley model compared to the power law model has less error in predicting gel simulant behavior, but at high shear rates, both models had a similar deviation from the experimental results. *Mallory et al*. [14] compared the rheological behavior of gel simulants (water and hydroxypropyl cellulose (HPC)) with Mono-Methyl Hydrazine (MMH) gel fuel. In this study, the simulants were prepared with 2-9 wt.% HPC, their behavior was compared with the rheological behavior of MMH with 4 wt.% HPC as a control sample. The results indicated that the gel simulant with 4 wt.% HPC has a similar behavior with MMH gel fuel.

Stiefel et al. [15] studied the gel simulant behavior in a nozzle (with a convergent section). Their experimental observations indicated that the gel simulant pressure drop is greater than the mother liquid. They also indicated that the maximum difference in a Newtonian fluid flow regime and the gel simulant flow occurs at the central part of the nozzle. *Mandal et al*. [16] studied the effect of injector geometry on the performance characteristics of a non-Newtonian fluid based on the power law model by using a 2D axisymmetric swirl simulation of a pressure swirl injector. They indicated that in shear-thinning fluids, discharge coefficient and spray cone angle decrease with increasing the swirl chamber diameter to injector orifice diameter ratio. *Rezaei Moghaddam et al*. [17] studied the behavior of non-Newtonian fluids in pressure swirl injectors based on the power law model using computational fluid dynamics. It was a two-dimensional axisymmetric swirl simulation with structural mesh and k-epsilon-RNG turbulence model. The results of their

study indicated that when the power law index (n) increases, the radial velocity of fluid decreases at the injector outlet. *Yang et al*. [18] investigated the effects of the geometry characteristics constant of pressure swirl injectors on the atomization of a gel simulant. They indicated that enhancement in the injector geometry characteristics constantly increased the breakup length, and spray cone angle, and decreased the discharge coefficient. *Kim et al*. [19] used a high-speed photograph system to study the atomization of kerosene, kerosene gel, and slurry kerosene in a pressure swirl injector. They showed that the breakup length and discharge coefficient for spraying slurry kerosene is higher than gel kerosene and liquid kerosene respectively. *Samanpour et al*. [20] using 3D simulations investigated the flooding phenomenon in brand-new designed fuel cells. They found that when the cross-section area reduces at a constant rate, the velocity increases significantly. In the lack of management, flooding will happen in cell fuels.

Fu et al. [21] examined the effect of the inlet diameter of an open-end pressure swirl injector on gel simulant atomization. They showed that when the diameter increases from 1.6 mm to 2 mm, the atomization process of the gel simulant improves. *Cho et al*. [22] investigated the effects of gellant concentration on the spray characteristics of a pressure swirl injector. A water-based non-Newtonian gel was used to simulate the cold-flow spray environment of a kerosene gel whose rheological properties were assessed. They indicated that the air core formation process in the gel simulant is similar to the Newtonian fluid. However, as the gellant content within the gel increased, the air core thickness decreased, so that a higher injection pressure was necessary to offset this discrepancy. *Sun et al*. [23] studied the atomization performance of GA (glycyrrhizic acid) hydrogel in impinging injectors and centrifugal injectors. They found that the spray pattern, breakup length of liquid film, and spray cone angle of 1.0% GA hydrogel were all similar to the pure water for two kinds of injectors, while the atomization performance degradation for 1.5% and 2.0% GA hydrogel.

Considering the importance of UDMH fuel, many investigations have been carried out on gelling UDMH fuel and improving it in terms of characteristics such as specific impulse, safety, and density. While few research works are available on the dynamic behavior and atomization of gel propellant; however, the suitable performance of the propulsion system is highly dependent on the dynamic behavior and atomization of the propellant. Also, no study has been done regarding the prediction of the dynamic behavior of gel fuel (as a shear-thinning fluid) in different parts of the gel propulsion system (pipeline, injector, and spray) using a comprehensive rheological model. Therefore, the main purpose of this paper is to select the most appropriate model among the various models of shear-thinning fluids to predict the dynamic behavior of UDMH-base gel fuel in a wide range of shear rates. Because in the pipeline, the shear rate is low and in the injector and spray mode, high shear rates are introduced into the gel. On the other side, the high toxicity of UDMH fuel makes the experimental tests of UDMH gel dynamic behavior and its atomization very difficult. Therefore, in the current work, the gel simulants are prepared from different gellants, and the dynamic behavior of the prepared gel simulants was compared to the base UDMH gel dynamic behavior (as control sample) in terms of power law model parameters and similarities in dynamic behavior between 0.21-21 1/s shear rates. The gel simulant with similar behavior of base UDMH gel was selected. Then, the behavior of the selected gel simulant was studied in a wide range of shear rates using different rheological models, and the most suitable rheological model was determined to predict the gelled propellant dynamic behavior. Eventually, the gelled propellant dynamic behavior and atomization characteris1tics were studied by computational fluid dynamics in a pressure swirl injector using the selected rheological model.

EXPERIMENTAL SECTION

Materials

In this study, methylcellulose (MC) (with 3500-5600 cP viscosity in 2% water at 20 ˚C), Carboxy Methyl Cellulose (CMC) (with 1500-3000 cP viscosity in 1% water at 25 ˚C), hydroxypropyl methylcellulose (HPMC) (with 100000 cP viscosity in 2% water at 20 ˚C) produced by Sigma Aldrich Co. were used. Distillate water was used to prepare the gel simulant.

Preparation of gel simulants

A cylindrical shape glass reactor with a 5 cm diameter and 14 cm length was used to prepare the gel simulants. The reactor lid had three openings; the middle opening was used for the mechanical stirrer, and the other two openings were the entries of the feed or used for placing a thermometer.

Table 1: List of investigated gel simulant compositions

Solvent (mother liquid)	Gellant	Gellant content (wt %)	Code
Distillate water	MC	2	MC-2%
Distillate water	MC	3	MC-3%
Distillate water	CMC	3	CMC-3%
Distillate water	CMC	3.5	CMC-3.5%
Distillate water	HPMC	0.85	HPMC-0.85%
Distillate water	HPMC	1	HPMC-1%

Furthermore, a magnetic heater-stirrer was utilized for temperature stabilization and better agitation. To prepare the gel simulants, first, 2/3 of the required distilled water was heated to 70-75 ˚C temperature, and then the gellant was gradually added. In this stage, the mixture was completely agitated with a mechanical mixer (with 400-450 rpm) and magnetic stirrer (in the opposite direction of the mechanical mixer) (with 400-500 rpm). Then, the rest of distilled water (1/3 of the total amount) was added to the solution at 5-10 ˚C, and the solution was mixed for 60-70 min, using a mechanical mixer (with 550-650 rpm) and a magnetic stirrer (with 700-800 rpm) to reach a homogenized mixture. Eventually, the solution was left for at least 12 hours until the completion of the gelation process. Table 1 shows the composition of the prepared gel simulants.

Dynamic behavior study

In this study, a Brookfield viscometer model DV-II-Pro was utilized to compare the dynamic behavior of the prepared gel simulants with the dynamic behavior of base UDMH gel and select the gel simulant with the maximum behavioral compliance with the base UDMH gel. The uncertainty of the Brookfield viscometer is 0.1 Pa.s. The apparent viscosity of the prepared gel simulants was measured by employing this device at the shear rate range of 0.2-21 1/s at 20 ˚C. To select the simulant gel with similar dynamic behavior of the base UDMH gel, the conformity of the power law model parameters, i.e., consistency index (K) and power index (n), were also used to investigate the dynamic behavior of the fluid. It should be noted that the viscosity of each sample was measured twice with the Brookfield device. Eq. (1) represents the relationship between the apparent viscosity and shear rate in the power law model.

$$\mu = K\dot{\gamma}^{n-1} \quad (1)$$

Where μ is the apparent viscosity in Pa.s, n is the fluid flow behavior index, K is the consistency index and $\dot{\gamma}$ is the applied shear rate on the fluid [12].

Rheological model study

Since the Brookfield viscometer cannot apply high shear rates, a rotating rheometer device, the Anton-Paar-MCR300 model, was used to select a suitable rheological model for the prediction of the dynamic behavior of UMDH gel fuel in a wide range of shear rates. The uncertainty of the Anton-Paar-MCR300 is 0.005 Pa.s. This rheometer consists of the cone-and-plate geometry with 0.05 mm gaps, 50 mm diameter. Different shear rates in the range of 0.001-1000 1/s were applied on the selected simulant gel by this device. According to the shear-thinning behavior of the UDMH gel propellant, in this section, the most suitable model was selected among the power law, Carreau-Yasuda, Cross and Carreau-bird models to predict the base UDMH gel fuel behavior. Equations (2) to (4) represent the Cross, Carreau-bird, and Carreau-Yasuda models, respectively [24]:

$$\frac{\eta(\dot{\gamma}) - \eta_\infty}{\eta_0 - \eta_\infty} = \frac{1}{1 + k(\dot{\gamma})^n} \quad (2)$$

$$\frac{\eta(\dot{\gamma}) - \eta_\infty}{\eta_0 - \eta_\infty} = [1 + (\dot{\gamma}\lambda)^2]^{\frac{n-1}{2}} \quad (3)$$

$$\frac{\eta(\dot{\gamma}) - \eta_\infty}{\eta_0 - \eta_\infty} = [1 + (\dot{\gamma}\lambda)^a]^{\frac{n-1}{a}} \quad (4)$$

In Eq. (2), η_∞ is the infinite-shear viscosity, η_0 is the zero-shear viscosity, n is the fluid flow behavior index, and K is the consistency index. In Eq. 3, $\eta(\dot{\gamma})$ is the apparent viscosity, η_∞ is the infinite-shear viscosity, η_0 is the zero-shear viscosity, and n is the power index. As shown in Eq. (4), the λ parameter is the time constant of the fluid response for changes in shear rate, and "a" parameter is the changes in the apparent viscosity curve due to variations in the shear rate at the transition zone from zero-shear

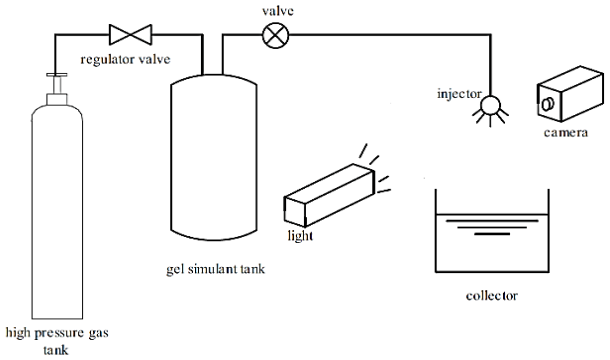

Fig 1: Schematic of the experimental setup

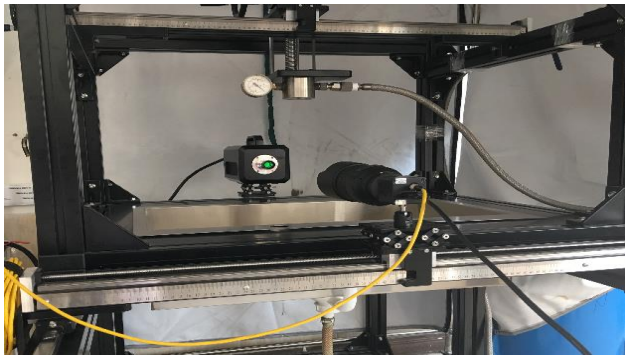

Fig 2: photograph system used in set-up

viscosity to the zone with a significant reduction in viscosity with shear rate [24, 25].

Injector test experimental system

A schematic of the experimental setup has been shown in Fig. 1. The experimental setup consists of a gel simulant tank, an injector unit, a pressure gauge and a camera. The measured data was recorded using a data acquisition system. A pressurized supply system was adopted. High-pressure gas forced the gel simulant to flow through the valve to the injector. The pressure inside the gel tank and the injector unit was monitored by pressure gauge whose the measuring range is 0–2.5 MPa. To visualize the spray, a camera was used and a 50 W lamp was used for the light source. The frame resolution was set at 504 × 504 pixels, and the shutter speed was set at 0.3 ms. Fig. 2. shows the injector test stand and photograph system.

THEORETICAL SECTION

Governing equations

The mass conservation or continuity (Eq. (5)) and the momentum or Navier-Stocks equation (Eq. (6)) are the governing equations for the flow simulation inside a pressure swirl injector. In Eq. (5), it is assumed that the density is constant and mass source and sink terms are neglected [26]. Also, the Volume of Fluid (VOF) model was employed to follow and capture the free surface between the air and the liquid phase inside the pressure swirl injector [27]. In the VOF model, the volume fraction of each phase in each computational cell is calculated from another equation called the volume fraction equation (Eq. 7).

$$\nabla . U = 0 \tag{5}$$

$$\frac{\partial U}{\partial t} + U.\nabla U = -\frac{1}{\rho}\nabla P + \frac{1}{\rho}\nabla.(2\mu D) + g + \frac{1}{\rho}F_b \tag{6}$$

$$f(x,t) = \begin{cases} 0 & \text{In gas} \\ 0 < f < 1 & \text{gas-liquid interface} \\ 1 & \text{In liquid} \end{cases} \tag{7}$$

In Equations (5) and (6), U, μ, P and ρ represent the velocity vector, fluid viscosity, pressure, and density, respectively. Also, "g" is the gravitational constant and F_b is the surface tension only at the two fluids interface. D represents the tension tensor (deformation). In Eq. (7), t is the time and x is the number of nodes in the numerical model. In the VOF method, the volume fraction of the first fluid in the cell is denoted as, for an empty cell; for a full cell and for partially filled with liquid, has a value between zero and one. In order to track the position of a free surface between two different phases additional advection equation for the additional phase was solved. The dependency of viscosity to shear rate in gel propellants is shear-thinning in dynamic mode; thus, the shear-thinning viscometric function are mostly used for the gel propellants. In this research, the Carreau-Yasuda model was used for modeling the viscosity. Using UDF (User Define Function), the Carreau-Yasuda model was compiled to the Fluent software. The fluid is shear-thinning non-Newtonian for n<1; Newtonian fluid for n = 1, is; and shear-thickening fluid for n > 1 [17].

Geometry and boundary conditions

The 3D modeling was used to study the effect of the rheological model on flow characteristics in a pressure swirl injector. Table 2 demonstrates the geometrical characteristics of the model and Fig. 3 shows a geometrical schematic of the studied model. The boundary conditions

Table 2: Configuration parameters of Pressure swirl injector

Characterization	Symbol	Value
Injector Length (mm)	L_T	8.75
Orifice Length (mm)	L_0	2
Orifice diameter (mm)	d_0	2
Swirl camber diameter (mm)	D_s	7
Swirl camber Length (mm)	L_s	4.25
Inlet diameter (mm)	d_p	2
Num. of inlet	-	2
Converge section angle (deg)	θ	45

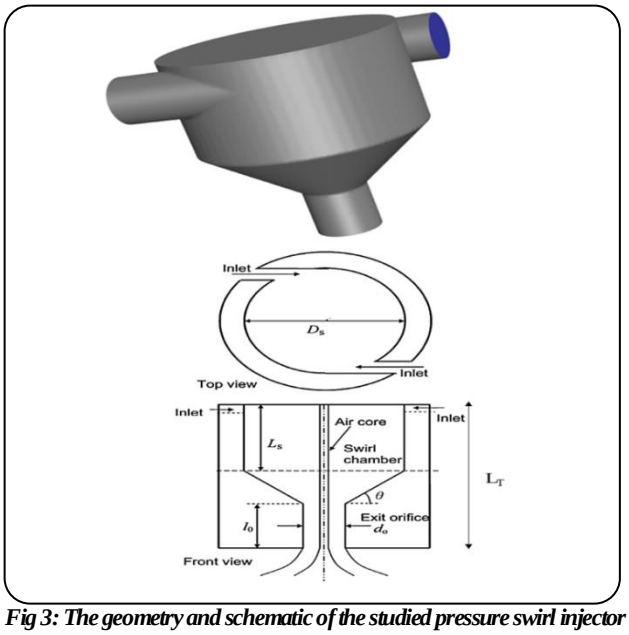

Fig 3: The geometry and schematic of the studied pressure swirl injector

for simulating the gel propellant as a working fluid in all the simulations are as follow:

- Pressure at the injector inlet (constant pressure of 1.4 MPa)
- Atmospheric pressure at the injector outlet (101.325 kPa)
- No–Slip boundary condition for the injector walls

Numerical method

The ANSYS software package of the FLUENT software was utilized for the numerical solution of flow inside the pressure swirl injector. To solve the two-phase field of the swirl injector, a pressure-based segregated algorithm was used. The SIMPLE algorithm was used to make the velocity field dependent on the pressure. The PRESTO! scheme was utilized for the interpolation of pressure on the surface of each cell because this method causes process stability in swirling flows. The second-order

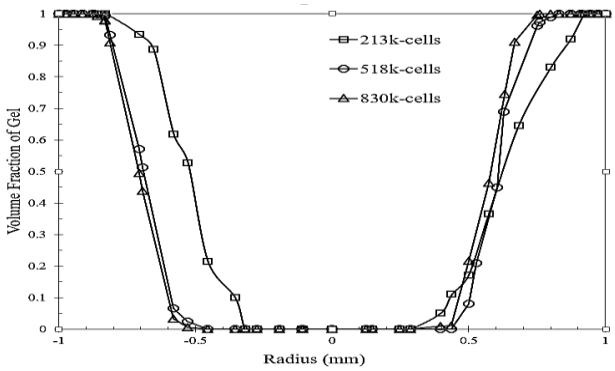

Fig 4: Mesh independence study in different distribution of mesh

upwind scheme was used to increase the accuracy of the momentum and turbulence equations (turbulence kinetic energy and rate of loss). The reason is that when the flow passes mesh lines obliquely, the first-order upwind scheme increases the numerical discretization error. Since the intense swirling of fluid around the injector axis develops significant pressure gradients inside the injector, the k-e-RNG turbulence model was utilized in pressure swirl injectors.

Mesh independency

Considering that the volume fraction of the sprayed fluid in the injector orifice is one of the most important parameters in swirl pressure injectors, this parameter is studied in this section for mesh independency. Fig. 4 indicates the volume fraction of the gel propellant along the injector orifice diameter at three computational cells of 213000, 518000, and 830000. The gel propellant volume fraction did not experience significant change by increasing the number of computational cells from 518000 to 830000 (Fig. 4); thus, 518000 computational cells were selected as the suitable number of computational cells.

Fig. 5 shows the meshing used for the simulation. As seen in Fig. 4, the injector's central axis area is dense due to the formation of an air core. Due to the strong pressure and velocity gradients, the boundary layer meshing with the value of y+=30 has also been conducted in the areas near the wall.

Validation

The experimental work of *Kim et al.* [19] was investigated to validate the selected solution method for the simulation. They tested a fuel with the thermophysical properties of 790 kg/m^3 density, 0.0024 Pa.s viscosity, and 0.027 N/m surface tension at room temperature and

Table 3: Error analysis of Numerical and experimental study

Pressure (MPa)	0.3	0.5	0.7	1
Exp (Mass Flow-g/s)	26.1	39.2	45.2	51.1
Num (Mass Flow-g/s)	28.7	37.1	41.9	47.9
|Error (%)|	9.96	5.83	7.31	6.26

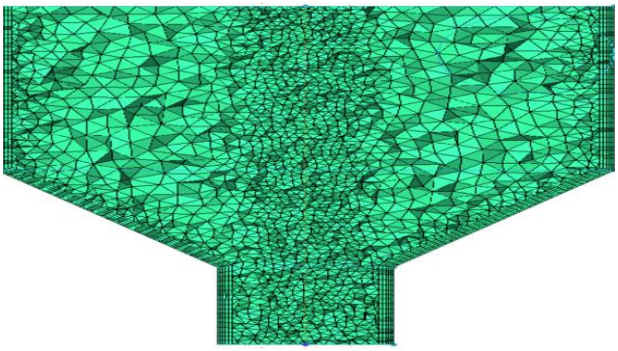

Fig 5: Sketch of the mesh used in present study

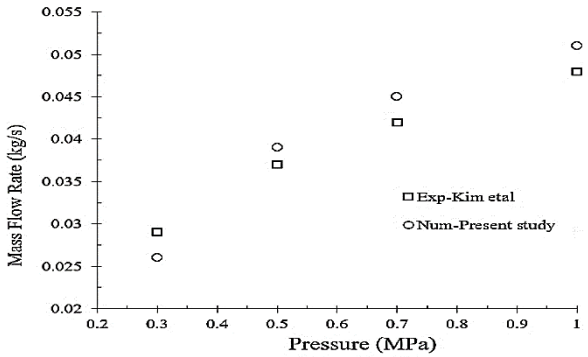

Fig 6: Validation of CFD results with experimental results

different injection pressures using a pressure swirl injector. The results of the numerical simulation and experimental test are compared in Fig. 6. Based on Table 3, the maximum error analysis of experimental and numerical study is 10%, indicating that the selected numerical method has a high confidence coefficient.

RESULTS AND DISCUSSION

The results of this investigation are presented in two sections: in the first section, the most suitable simulant was selected by comparing the dynamic behavior of the gel simulants and base UDHM gel, then the suitable rheological model was used to predict the gel fuel behavior in a wide range of shear rates. In the second section, the selected rheological model in section 1 was utilized to simulate the gel flow inside a pressure swirl injector and investigate the gel flow characteristics.

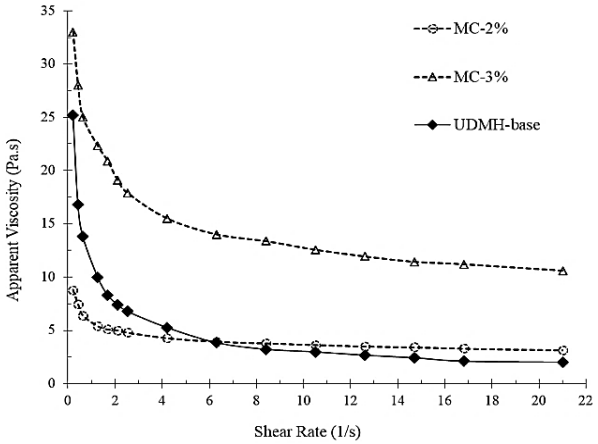

Fig 7: Comparison of the dynamic behavior of basic UDMH gel with MC-2% and MC-3% at 20 °C

Selecting the appropriate simulant gel

According to Table 1, the dynamic behavior of the gel simulant samples prepared by adding different percentage of gellants was separately compared with base UDMH gel dynamic behavior.

I-Gel simulants containing MC

Fig. 7 shows the changes in apparent viscosity as a function of shear rate for the prepared gel simulants from MC gellant and base UDMH. These curves indicate that all three samples have shear-thinning behavior, and the apparent viscosity of gel simulant increases by methylcellulose concentration enhancement. Considering that the number of methyl cellulose chains increases in water by increased methylcellulose concentration, the apparent viscosity of the solution increases [28].

By comparing the decreasing trend of the apparent viscosity of MC-3% and MC-2% with increasing shear rate, it can be concluded that with the increase of shear rate due to more breaking of the formed chains, the decreasing trend of MC-3% is more than MC-2%. In addition to the mentioned results, the base UDHM gel curve and MC-3% and MC-2% simulant curves show that the apparent viscosity reduction rate in base UDHM gel is greater than the MC made simulants at increased shear rates. Table 4 demonstrates the K and n values obtained from the curve fitting of the power law model for base UDHM gel and the simulants prepared by MC. As seen in Fig. 7, the behavior of the gel simulants prepared by 2 and 3 wt% of MC is different from the base UDHM gel behavior. Furthermore, the data in Table 4 indicate that the K and n values of the UDHM

Table 4: Comparison of n and K of MC-2% and MC-3% with basic UDMH gel at 20 °C

Consistency index (K) Pa.s^n			Power law index (n)		
UDMH	MC-2%	MC-3%	UDMH	MC-2%	MC-3%
10.8	5.9	22.7	0.44	0.79	0.75

Table 5: Comparison of n and K of CMC-3% and CMC-3.5% with basic UDMH gel at 20 °C

Consistency index (K) Pa.s^n			Power law index (n)		
UDMH	CMC-3%	CMC-3.5%	UDMH	CMC-3%	CMC-3.5%
10.8	7.7	18.8	0.44	0.68	0.58

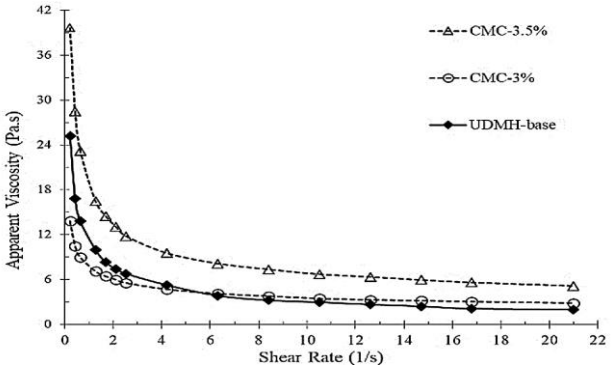

Fig 8: Comparison of the dynamic behavior of basic UDMH gel with CMC-3% and CMC-3.5% at 20 °C

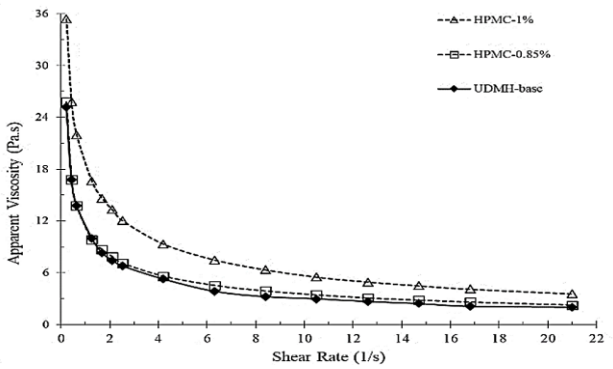

Fig 9: Comparison of the dynamic behavior of basic UDMH gel with HPMC-0.85% and HPMC-1% at 20 °C

gel have significant differences with MC gel simulants data. Thus, it can be concluded that the gel simulant made from MC, with both compositions, cannot show a behavior similar to base UDHM gel.

II- Gel simulants containing CMC

In this section, a comparison is done between the apparent viscosity changes with enhanced shear rate applied on the base UDHM gel and the gel simulants containing CMC wt% 3 and 3.5 wt.%. Fig. 8 indicates that the changing trend of the CMC-3.5 % is similar to the base UDMH gel, but they differ in terms of apparent viscosity at high and low shear rates. Also, CMC-3% gel simulant in terms of apparent viscosity at low shear rates is lower than base UDMH gel viscosity. At high shear rates, it has a higher apparent viscosity than base UDMH, indicating the less shear-thinning behavior of this simulant compared to the base UDMH gel.

Considering the apparent viscosity changing trend, it can be expressed that the gel simulant with 3.5 wt% CMC has similar behavior with the base UDMH gel; however, to make an accurate decision in selecting a suitable gel simulant using the power law model, it is necessary to study the consistency and the flow behavior indices. The values of n and K parameters obtained from the curve-fitting of the power law model for the base UDMH gel and the prepared simulants with CMC gellant are listed in Table 5. Based on the data in Table 5, the values of n and K parameters for the gel simulant containing CMC 3 wt% have significant differences with the base UDMH gel parameters. Despite the rather similar behavior of the gel simulant containing CMC 3.5wt% with the UDMH gel behavior, their values of K and n constants are not matched.

III- Gel simulants containing HPMC

Fig. 9 shows the trend of the apparent viscosity changes when the shear rate increases for the gel simulants containing HPMC 0.85 and 1 wt% compared to the base UDMH gel behavior. The apparent viscosity change curve as a function of shear rate enhancement indicates that the behavior of both simulants is similar to the base UDMH gel, But the gel simulant containing HPMC 0.85 wt% in addition to the similar trend, has apparent viscosity values close to the base UDMH gel at identical shear rates.

The values of n and K for the base UDMH gel and gel simulants made from HPMC are compared in Table 6. According to data presented in Table 6, the simulant gel containing HPMC 1 wt% has the closest value of flow

Table 6: Comparison of n and K of HPMC-0.85% and HPMC-1% with basic UDMH gel at 20 °C

Consistency index (K) Pa.s^n			Power law index (n)		
UDMH	HPMC-3%	HPMC-3.5%	UDMH	HPMC-3%	HPMC-3.5%
10.8	7.7	18.8	0.44	0.68	0.58

Table 7: The R-squared obtained from the rheometry data fittings for different models for the rheometry of the HPMC-0.85% at 20 ˚C

Rheological model	Carreau-Yasuda	Carreau-bird	Cross	Power law
R-Squared (R^2)	0.999	0.996	0.988	0.939

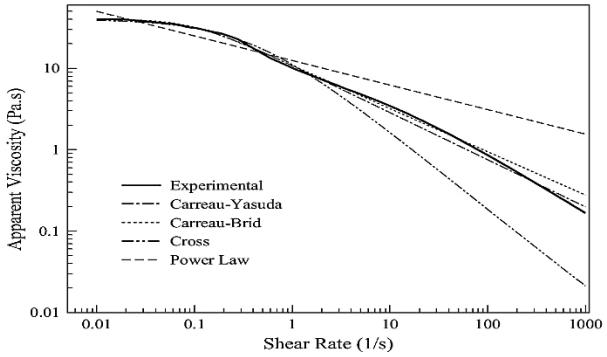

Fig. 10: Curve fitting of the HPMC-0.85% with different rheological models at 20 ˚C

behavior index to the base UDMH gel. However, the consistency index and initial viscosity of the simulant gel with HPMC 1 wt% are much higher than the base UDMH gel. Finally, based on the trend of changes in the apparent viscosity of the simulant gel containing HPMC 0.85 wt % (Fig. 9) and its n and K values, and comparing them with those for the base UDMH gel, it can be concluded that this simulant has more similar behavior to the base UDMH gel than other made simulant gels. Therefore, it was selected as the suitable simulant.

Selecting the suitable rheological model

The curve fitting results of the experimental data with four models, including power law, cross, Carreau-bird, and Carreau-Yasuda is illustrated in Fig. 10. The selected gel experimental curve (the solid line) in Fig. 10 shows that the selected gel simulant has zero-shear viscosity at the shear rate range of 0.01-0.07 1/s due to a small change in the viscosity value. However, the apparent viscosity of the selected gel simulant decreased sharply at the shear-thinning area.

According to Fig. 10, the power law and cross models cannot predict the gel simulant behavior at the applied shear rate range. The cross model could well predict the behavior of the gel simulant containing HPMC 0.85 wt% at low shear rates, but it does not have good compliance with the dynamic behavior of the selected gel simulant at high shear rates. The power law model not only could not predict the dynamic behavior of the selected simulant at high shear rates but also could not predict it at low shear rates. The reason is that there is no parameter in the power law model to determine the zero-shear viscosity, and it is mostly used in the shear-thinning region.

The Carreau-Yasuda and Carreau-bird models had good compliance with the selected simulant behavior at almost all the applied shear rate ranges. The reason is that both models have parameters for predicting the apparent viscosity at zero-shear viscosity regions. However, a deep look indicates that the Carreau-Yasuda had a better prediction than the Carreau-bird model at high shear rates and has a more precise curve fitting. The R-squared (R^2) of the curve fittings are listed in Table 7 for a better decision. The data in this Table indicate that the R-squared of the Carreau-Yasuda model is closer to 1 compared to the other models. Therefore, it has higher accuracy in predicting the selected gel simulant behavior.

Based on the selection of the Carreau-Yasuda model as the most suitable rheological model for predicting the UDHM gel simulant behavior, the values of the Carreau-Yasuda parameters are calculated from Eq. (4) after the curve fitting of the experimental data and are presented in Table 8. It should be noted that since the reference solvent for the preparation of the gel simulant with 0.85 wt% of HPMC was water, the infinite shear-viscosity value (η_∞) of this model was considered the viscosity of water.

Investigating the flow characteristics of swirl pressure injector

In this section, the flow characteristics of the swirl pressure injector including spray angle, mass flow rate, and discharge coefficient obtained from experimental tests and the simulation of the gel simulant are compared and the dynamic flow pattern of the simulant inside the injector is studied.

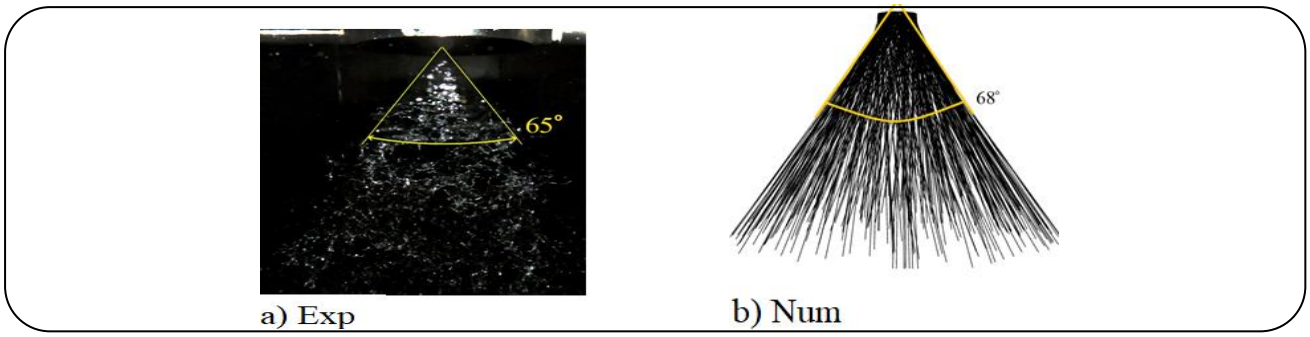

Fig 11: Spray cone angle of simulant gel a) Experimental b) numerical under the pressure drop of 1.4 MPa

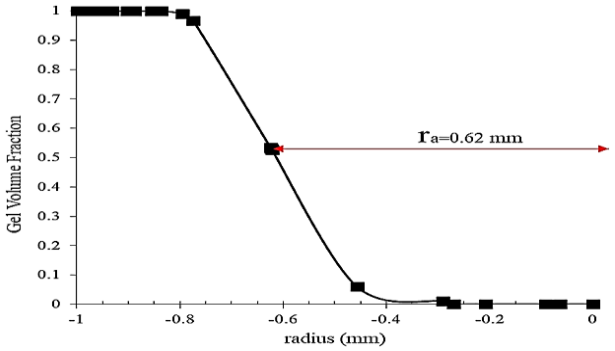

Fig 12: Volume fraction of gel in injector outlet

I- The spray cone angle

One of the important parameters in the determination of the pressure swirl injector performance is the output fluid spray cone angle. Fig. 11-a shows the spray cone angles of the gel simulant obtained from the pressure swirl injector, based on the dimensions in Table 2, at the injection pressure of 1.4 MPa. Although precise measurement of the spray cone angle in the experimental test is difficult due to the pulses, the spray cone angle of 65 was obtained after several measurements. On the other side, since the spray angle is dependent on the angle and direction of the velocity vector at the injector output, Fig. 11-b shows the extension of the flow velocity vector obtained from the numerical simulation at the outlet of the injector at 1.4 MPa. The values obtained from the experimental test and numerical simulation show that using Carreau-Yasuda rheological model (based on the constants listed in Table 8), the spray cone angle could be predicted with less than 5% error.

II- Mass flow rate and discharge coefficient

Table 9 presents the mass flow rate and discharge coefficient obtained from the experimental test and numerical simulation at 1.4 MPa operation condition. Based on the definition of discharge coefficient, which is the ratio of the real flow rate to the ideal flow rate, it can be calculated from Eq. 8.

$$C_d = \frac{\dot{m}_{Exp\ or\ Num}}{\dot{m}_{ideal}} = \frac{\dot{m}_{Exp\ or\ Num}}{A_n\sqrt{2\rho\Delta p}} \quad (8)$$

In Eq. (8), A_n is the injector orifice cross-sectional area, ρ is the fluid density, and Δp is the injection pressure. By comparing the results of the experimental and numerical simulation, it is concluded that the dynamic behavior of the gel can be predicted by using the Carreau-Yasuda rheological model, in terms of determining the operating conditions and flow rate. Also, the surface filling factor which indicates the ratio of the occupied surface by the gel is calculated from Eq. 9, using the numerical results.

$$\text{surface filling factor} = 1 - \frac{r_a^2}{r_n^2} \quad (9)$$

In Eq. 9, r_a is the radius of the air core formed in the injector orifice, and r_n is the injector orifice radius. Fig. 12 shows the gel volume fraction at the injector outlet. As seen in this Fig, the volume fraction of 0.5 is considered as the gel and air phase separation region, and the radius of the air core was calculated accordingly. The surface filling factor indicates that about 61% of the injector orifice surface was occupied by the gel.

III- Gel simulant flow pattern

Fig. 13 shows the volume fraction contour of the gel simulant. As seen in this Figure, the air core is formed at the central axis of the injector. To justify this phenomenon, it can be concluded that the formation of the air core in a pressure swirl injector is the result of the centrifuge force (created by swirl speed) overcoming the viscous force, and the negative pressure region forms in the central axis of the injector.

Table 8: Carreau-Yasuda parameters for selected gel simulant (HPMC-0.85%)

Carreau-Yasuda parameters	Value
a	1.58
λ (s)	9.48
n	0.42
η_0 (Pa.s)	40
η_∞ (Pa.s)	0.001

Table 9: Comparison of mass flow rate and discharge coefficient obtained from simulation with experimental results

Characterization	Exp	Num	Error (%)
Mass flow rate (gr/s)	63.8	60.1	5.7
Mass flow rate (gr/s)	166.1	166.1	-
Discharge Coefficient	0.384	0.362	5.8
Surface filling factor	-	0.61	-

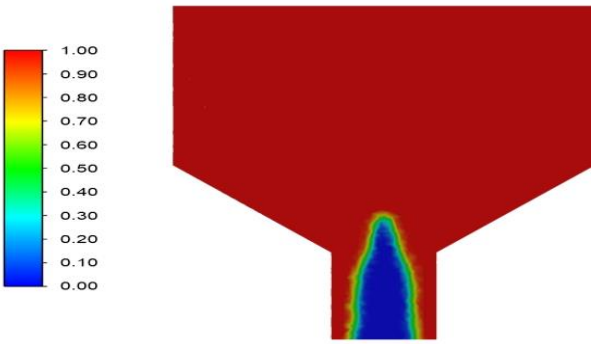

Fig. 13: Gel propellant volume fraction contour

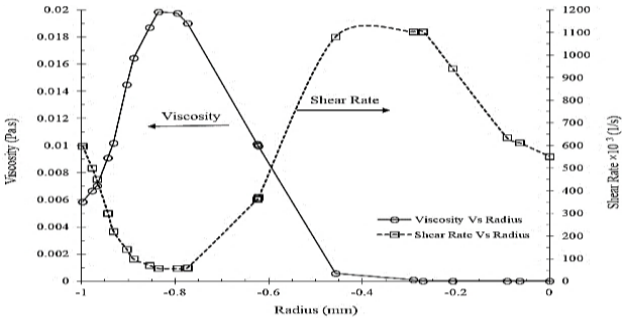

Fig. 14: Viscosity and shear rate changes versus injector orifice radius

According to Figs 13 and 14, which show the viscosity and shear rate as a function of the radius of the injector orifice, it is evident that with the increase of the shear rate near the injector wall, the viscosity of the simulant gel decreased due to the shear-thinning behavior and it has reached a viscosity of 0.006 Pa.s. Therefore, as a result of the reduction in gel simulant viscosity at the injector outlet, the centrifugal force overcomes the viscous force and creates a negative pressure region at the central axis of the injector and pulling the ambient air into the injector.

Fig. 15 also shows the streamlines inside the injector. It is evident that inside the swirl chamber of the injector, the swirling speed is the dominant speed on the gel flow, so the swirling speed causes a vortex in the swirl chamber of the injector. On the other hand, as the gel moves toward the injector outlet, the cross-section area of flow reduces and the swirling speed changes into the axial speed, which reduces the flow turbulence.

CONCLUSIONS

In this research, the dynamic behavior of gel simulants prepared with different compositions from methylcellulose, carboxymethyl cellulose, and hydroxyl propyl methyl cellulose as gallant agents was compared to the dynamic behavior of the base UDHM gel, and the appropriate gel simulant was selected. Then, to predict the base UDMH gel behavior, the behavior of the selected gel was studied in a wide range of shear rates, and a suitable rheological model was selected among different models. Eventually, the dynamic behavior of the selected gel simulant was simulated inside the pressure swirl injector using the selected rheological model and the results of this numerical simulation were compared to the experimental test results. Some of the most important results of this investigation are summarized in the following:

- The prepared simulant gels from methylcellulose and carboxy methyl cellulose at different compositions had less shear-thinning behavior than the base UDMH gel.

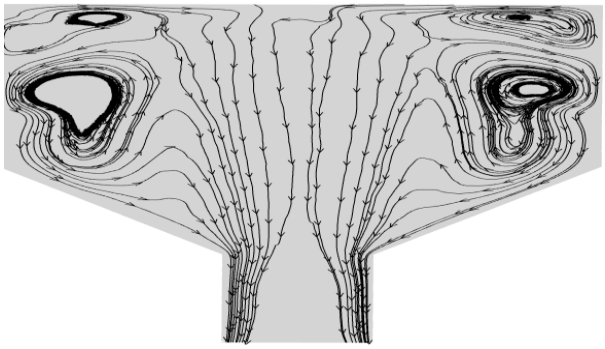

Fig. 15: streamlines inside the injector

• The simulant gel with HPMC 0.85 wt% was selected as the most suitable gel due to the compliance of its dynamic behavior under enhanced shear rate and the vicinity of its power law index with the base UDMH gel.

• The investigation of the gel simulant rheometry showed that among the power law, cross, Carreau-Bird, and Carreau-Yasuda models, the Carreau-Yasuda can predict the selected gel simulant dynamic behavior in a wide range of shear rates.

• A comparison of the experimental results and the numerical simulation results of the gel simulant inside the pressure swirl injector indicated that the dynamic behavior of the gel simulant, especially its functional characteristics of mass flowrate, discharge coefficient, and spray cone angle can be predicted well by the constants obtained from the Carreau-Yasuda model.

• Results of numerical simulation with the Carreau-Yasuda model showed that the simulant gel viscosity decreases to 0.006 Pa.s near the outlet orifice wall of the injector when the injection pressure is 1.4 MPa.

In conclusion, it is recommended to investigate the effect of dimensionless design parameters such as the orifice Length/Diameter ratio, the swirl chamber Length/Diameter ratio, and the convergence angle of the spray gel.

Abbreviations

MC	Methyl cellulose
CMC	Carboxymethylcellulose
HPMC	hydroxypropyl methylcellulose
UDMH	Unsymmetrical dimethylhydrazine
MMH	Monomethylhydrazine
HPC	Hydroxypropyl cellulose
UDF	User Define Function

Nomenclature

Symbol	Meaning
μ	Apparent viscosity, Pa.s
K	Consistency index, Pa.s^n
n	Fluid flow behavior index
$\dot{\gamma}$	Shear rate, 1/s
η_0	Zero-shear viscosity. Pa.s
η_∞	Infinite-shear viscosity. Pa.s
λ	Time constant. s
$\eta(\dot{\gamma})$	Apparent viscosity, Pa.s
a	Shear rate at the transition zone
U	Velocity vector
g	Gravity, m/s^2
F_b	Surface tension, N/m
ρ	Density, kg/m^3
f (x,t)	Volume fraction
$\dot{m}$	Mass flow rate, kg/s
A_n	Nozzle surface area, m^2
r_a	Air core radius, m
r_n	Injector orifice radius, m
D	Tension tensor

Received : Jan. 05, 2023 ; Accepted : Apr. 24, 2023

REFERENCE

[1] Wang F., Chen J., Zhang T., Guan H., Li H., Experimental Study on Spray Characteristics of ADN/Water Based Gel Propellant with Impinging Jet Injectors, *Propellants, Explosives, Pyrotechnics*, **45**: 1357-1365 (2020).

[2] Rahimi S., Peretz A., Natan B., On Shear Rheology of Gel Propellants, *Propellants, Explosives, Pyrotechnics*, **32**: 165-174 (2007).

[3] Varma M., High Shear Rheometry of Unsymmetrical Dimethylhydrazine Gel, *Chemical Rocket Propulsion. Springer*, 519-542 (2017).

[4] Gupta B., Varma M., Munjal N., Rheological Studies on Virgin and Metallized Unsymmetrical Dimethyl Hydrazine Gelled Systems, *Propellants, Explosives, Pyrotechnics*, **11**: 45-52 (1986).

[5] Padwal M.B., Natan B., Mishra D., Gel Propellants, *Progress in Energy and Combustion Science*, **83**: 100885 (2021).

[6] Saberi M.A., Rezaei M.R., Tavangar S. Experimental Investigation of Characteristic Length Influence on a Combustion Chamber Performance with Liquid and Gelled UDMH/IRFNA Bi-Propellants, *Propellants, Explosives, Pyrotechnics*, **44**: 1154-1159 (2019).

[7] Yoon C., Heister S. D., Xia G. Merkle C. L., Numerical Modeling of Injection of Shear-Thinning Gel Propellants Through Plain-Orifice Atomizer, *Journal of Propulsion and Power*, **27**: 944-954 (2013).

[8] Baek G., Kim S., Han J., Kang C. K., Atomization Characteristics of Impinging Jets of Gel Material Containing Nanoparticles, *Journal of Non-Newtonian Fluid Mechanics*, **166**: 1272-1285 (2011).

[9] Ciezki H. K., Naumann K. W., Some Aspects on Safety and Environmental Impact of the German Green Gel Propulsion Technology, *Propellants, Explosives, Pyrotechnics*, **41**: 539-547 (2016).

[10] Li M. G., Wu Y., Cao L., Yuan Y., Chen X., Han J., Wu W., Rheological Properties of Organic Kerosene Gel Fuel. *Gels*, **8**: 507-519 (2022).

[11] Yoon, C., Heister S. D., Xia G., Merkle C. L., "Numerical Simulations of Gel Propellant Flow Through Orifices", *45th AIAA/ASME/SAE/ASEE Joint Propulsion Conference & Exhibit*, 50-61 (2009).

[12] Madlener K., Ciezki H.K., Estimation of Flow Properties of Gelled Fuels with Regard to Propulsion Systems, *Journal of Propulsion and Power*, **28**: 113-121 (2012).

[13] Jyoti B., Varma M., Baek S.W., "Comparative Study of Rheological Properties of Ethanol and UDMH Based Gel Propellants", *5th European Conference for Aeronautics and Space Sciences*, 70-86 (2013).

[14] Mallory J., Sojka P., "Jet Impingement and Primary Atomization of Non-Newtonian Liquids", PhD Thesis, Purdue University (2012).

[15] Stiefel A.D., Kirchberger C. U., Ciezki H. K., Kurilov M., Kurth G., The Flow of Gels Through a Nozzle Like Geometry, *International Journal of Energetic Materials and Chemical Propulsion*, **19**: 21-33 (2020).

[16] Mandal A., Jog M.A., Xue J., Ibrahim A.A., Flow of Power-Law Fluids in Simplex Atomizers, *International Journal of Heat and Fluid Flow*, **29**: 1494-1503 (2008).

[17] Rezaeimoghaddam M., Elahi R., Modarres Razavi M.R., Ayani, M.B. Modeling of Non-Newtonian Fluid Flow Within Simplex Atomizers, *Engineering Systems Design and Analysis*, **49170**: 549-556 (2010).

[18] Yang L. J., Fu Q. F., Qu Y. Y., Zhang W., Du M. L., Xu B. R., Spray Characteristics of Gelled Propellants in Swirl Injectors, *Fuel*, **97**: 253-261 (2012).

[19] Kim H., Ko T., Kim S., Yoon W., Spray Characteristics of Aluminized-Gel Fuels Sprayed Using Pressure-Swirl Atomizer, *Journal of Non-Newtonian Fluid Mechanics*, **249**: 36-47 (2017).

[20] Samanipour H., Ahmadi N., Jabbary A., Effects of Applying Brand-New Designs on the Performance of PEM Fuel Cell and Water Flooding Phenomena, *Iranian Journal of Chemistry and Chemical Engineering (IJCCE)*, **41**: 618-635 (2022).

[21] Fu Q., Ge F., Wang W., Yang L., Spray Characteristics of Gel Propellants in an Open-End Swirl Injector, *Fuel*, **254**: 115555-115565 (2019).

[22] Cho J., Lee D., Kang T., Moon H., Study on Spray Characteristics of Simulant Gel in Pressure Swirl Injector, *International Journal of Aeronautical and Space Sciences*, **23**: 794–803 (2022).

[23] Sun H., Jian J., Li Zh., Yuan Ch., Liu P., Jiang Y., Rheological and Atomization Behavior of Glycyrrhizic Acid Based Supramolecular Gel Propellant Simulant, *Colloids and Surfaces A: Physicochemical and Engineering Aspects*, **640**: 128460 (2022).

[24] Morrison F.A., "Understanding Rheology", Oxford University Press, (2001).

[25] Chhabra R.P., Richardson J.F., "Non-Newtonian Flow and Applied Rheology: Engineering Applications", Butterworth-Heinemann, (2011).

[26] Ahmadi N., Rezazadeh S., Asgharikia M., Shabahangnia E., Optimization of Polymer Electrolyte Membrane Fuel Cell Performance by Geometrical Changes, *Iranian Journal of Chemistry and Chemical Engineering (IJCCE)*, **36(2)**: 89-106 (2017).

[27] Baek G., Kim S., Han J., Kang C. K., Review on Pressure Swirl Injector in Liquid Rocket Engine, *Acta Astronautica*, **145**: 174-198 (2018).

[28] Jung H.S., Kim H.C., Park W.H., Robust Methylcellulose Hydrogels Reinforced with Chitin Nanocrystals, *Carbohydrate Polymers*, **213**: 311-319 (2019).